

Supporting Information

**Bare and sterically stabilized PLGA nanoparticles
for the stabilization of Pickering emulsions**

Claire Albert^a, Nicolas Huang^{a}, Nicolas Tsapis^a, Sandrine Geiger^{a, b}, Véronique Rosilio^a,
Ghozlene Mekhloufi^a, David Chapron^a, Baptiste Robin^a, Mohamed Beladjine^a, Valérie Nicolas^c,
Elias Fattal^a, Florence Agnely^a*

^a Institut Galien Paris-Sud, CNRS UMR 8612, Univ Paris-Sud, Université Paris-Saclay, Faculté
de Pharmacie, 5 rue J.B. Clément, 92296 Châtenay-Malabry, France.

^b Laboratoire Structures, Propriétés et Modélisation des Solides (SPMS), UMR CNRS 8580,
CentraleSupélec, Université Paris-Saclay, 3 Rue Joliot Curie, 91190 Gif-sur-Yvette, France.

^c Plateforme d'imagerie cellulaire MIPSIT, SFR-UMS-IPSIT, Univ. Paris-Sud, Université Paris-
Saclay, Faculté de Pharmacie, 5 rue J.B. Clément, Châtenay-Malabry F-92296, France

**Corresponding Author: N. Huang nicolas.huang@u-psud.fr*

TABLE OF CONTENT

Supporting Information 1: NP preparation..... 3

Supporting Information 2: Amount of PVA adsorbed on the surface of the NPs..... 5

Supporting Information 3: Characterization of PLGA-PVA NP surface 7

Supporting Information 4: AFM imaging of the layers of NPs 11

Supporting Information 5: NP hydrophobicity measurements 15

Supporting Information 6: Examples of Turbiscan curves obtained for the emulsion stabilized by lyophilized PLGA-PVA NPs 19

Supporting Information 7: Comparison of the stability of emulsions stabilized either by lyophilized PLGA-PVA NPs, non-lyophilized PLGA-PVA NPs, or trehalose solution 21

Supporting Information 8: Confocal microscopy images of emulsions for different water/oil ratios..... 23

Supporting Information 9: Values of interfacial tension and interfacial moduli at 12 h 25

Supporting Information 10: Modeling of the adsorption kinetics of NPs at the oil/water interface..... 26

Supporting Information 11: Measurement of the critical aggregation concentration (CAC) of PVA..... 31

Supporting Information 1: NP preparation

PLGA-PVA NPs stabilized by using poly(vinyl alcohol) (PVA) were prepared according to the previously described emulsion-evaporation method.¹ Briefly, 100 mg of PLGA were dissolved in a 5 mL dichloromethane/acetone (1/1 v/v) mixture and pre-emulsified by vortexing for 1 min with 20 mL of an aqueous solution containing 2.5 mg/mL of PVA. This pre-emulsion was kept in ice and immediately sonicated (VibraCell sonicator, Fisher Scientific, France) at a power of 40% for 1 min. The organic solvent was then evaporated at room temperature under magnetic stirring for 2 h. After evaporation, MilliQ water was added to the NP suspension up to a volume of 20 mL. Purification of NPs was achieved by ultracentrifugation (LE-80K Ultracentrifuge Beckman Coulter Optima™) at 4 °C, 37,000 g for 1 h. After elimination of the supernatant, the NPs were re-suspended in 4 mL of MilliQ water, up to a concentration of 25 mg/mL, when they were not lyophilized. For NPs subsequently lyophilized, this step was replaced by a resuspension in 12 mL of an aqueous solution containing 50 mg/mL of trehalose (cryoprotectant) using an ultrasound bath for 15 min. Then, the NP suspension was frozen with liquid nitrogen before being lyophilized (Alpha 1–2 LO plus Bioblock Scientific, 24 h, 0.5 mbar, – 55 °C). Before use, lyophilized NPs were redispersed in MilliQ water at 25 mg/mL.

PLGA NPs were prepared, without any other polymer or surfactant, according to a nanoprecipitation method previously described.² Briefly, 150 mg of PLGA were dissolved in 15 mL of acetonitrile. This solution was added dropwise at 7 mL/min with a syringe pump (Harvard Apparatus 11 plus, Holliston, USA) into 45 mL of MilliQ water under magnetic stirring.

The suspension was kept under magnetic stirring for one minute once the addition of the organic phase was ended. Then, the organic solvent was evaporated and the suspension concentrated by evaporation of water under reduced pressure at 39 °C with a rotary evaporator, up to a final volume of 6 mL corresponding to a theoretical NP concentration of 25 mg/mL. The solid content in the suspension was estimated according to the volume of the suspension and the mass of polymer initially introduced.

REFERENCES

- (1) Mura S.; Hillaireau H.; Nicolas J.; Le Droumaguet B.; Gueutin C.; Zanna S.; Tsapis N.; Fattal E. Influence of Surface Charge on the Potential Toxicity of PLGA Nanoparticles towards Calu-3 Cells. *Int. J. Nanomedicine* **2011**, 2591.
- (2) Grabowski, N.; Hillaireau, H.; Vergnaud, J.; Tsapis, N.; Pallardy, M.; Kerdine-Römer, S.; Fattal, E. Surface Coating Mediates the Toxicity of Polymeric Nanoparticles towards Human-like Macrophages. *Int. J. Pharm.* **2015**, 482 (1–2), 75–83.

Supporting Information 2: Amount of PVA adsorbed on the surface of the NPs

The amount of PVA adsorbed at the PLGA-PVA NP surface, during the emulsion-evaporation process, was indirectly measured by determining the PVA concentration in the supernatant after the centrifugation step described in Supporting Information 1. The amount of PVA possibly desorbed from the NP surface after resuspension was measured by determining its concentration in the supernatant after a second centrifugation of the PLGA-PVA NPs re-dispersed in 3 mL of MilliQ water. A spectroscopic method based on the formation of a green-colored complex between PVA and iodine in presence of boric acid was used to quantify PVA.¹ The supernatant was diluted with water so that PVA concentrations were within the range of the calibration curve (5 to 50 µg/mL of PVA). Then, 3 mL of a boric acid solution (3.8% w/v) and 0.6 mL of an iodine solution (1.27% w/v of iodine and 2.5% w/v of potassium iodide) were added. The volume was adjusted to 10 mL with water. The absorbance of the final solution was measured at 650 nm using the solution of boric acid and aqueous iodine as a reference.

The amount of PVA associated to PLGA-PVA NPs was quantified by the difference between the amount of PVA initially introduced and the amount of free PVA in the supernatant after the first centrifugation step. This quantification showed that 2 mg of PVA were associated to 25 mg of PLGA-PVA NPs corresponding to 8% (w/w of PLGA) of PVA in PLGA-PVA NPs, in agreement with the previous work of Mura *et al.*² After a second centrifugation step, 150 µg of these 2 mg of PVA were titrated in the supernatant. Thus, the quantity desorbed from the NPs was not significant.

In this work, it was considered, in a first approximation, that there was no free PVA chains present in the PLGA-PVA NPs aqueous suspension. Moreover, according to the Supporting Information 3, the 8% of PVA chains in the PLGA-PVA NPs were found to be exclusively at the NP surface.

REFERENCES

- (1) Joshi, D. P.; Lan-Chun-Fung, Y. L.; Pritchard, J. G. Determination of Poly (Vinyl Alcohol) via Its Complex with Boric Acid and Iodine. *Anal. Chim. Acta* **1979**, *104* (1), 153–160.
- (2) Mura S.; Hillaireau H.; Nicolas J.; Le Droumaguet B.; Gueutin C.; Zanna S.; Tsapis N.; Fattal E. Influence of Surface Charge on the Potential Toxicity of PLGA Nanoparticles towards Calu-3 Cells. *Int. J. Nanomedicine* **2011**, 2591.

Supporting Information 3: Characterization of PLGA-PVA NP surface

The aim of this experiment was to determine the composition of PLGA-PVA NP surface. Does it solely consist of PVA, PLGA or both? To answer this question, the PLGA-PVA NP interface during NP preparation by the emulsification-evaporation process was mimicked and analyzed by interfacial tension measurements.

To characterize the surface of PLGA-PVA NPs, interfacial tension measurements were performed using a pendant drop tensiometer (Tracker, Teclis, France, with 18 G straight needle and 100 μ L syringe). The PLGA-PVA NP interface during their formation using the emulsification-evaporation process was mimicked by forming a drop of a dichloromethane/acetone (1/1 v/v) mixture, containing or not PLGA at 20 mg/mL, into water, containing or not PVA at 2.5 mg/mL. The same system without acetone was also studied to assess the influence of this solvent. The interfacial tension was measured at 1 min because the droplet quickly detached from the needle in the presence of acetone and PVA (the minimal surface tension at which detachment took place being 2 mN/m for the used needle and droplet volume). The measurement was performed with a droplet of 5 μ L at 20 °C from at least five independently formed drops. In presence of PVA in the cuvette and without acetone in the droplet, the detachment occurred immediately, so that no measurement was possible.

Interestingly, PLGA chains had a slight interfacial activity at the dichloromethane/water interface (*i.e.* without acetone). Indeed, the interfacial tension decreased from 25.6 ± 0.3 mN/m to

22.1 ± 0.4 mN/m (Table S3). This result was consistent with previous observations from Pisani *et al.*¹ who showed that PLGA chains were able to adsorb at the dichloromethane/water interface. This slight interfacial activity was not observed in the presence of acetone in the organic phase, meaning that PLGA was not able to adsorb at the interface in these conditions.

Drop phase	Cuvette phase	Interfacial tension (mN/m)	
		Water	Water + PVA ^d
Dichloromethane		25.6 ± 0.3	na
Dichloromethane + PLGA^a		22.1 ± 0.4	na
Dichloromethane + acetone^b		22.4 ± 0.8	5.2 ± 0.2
Dichloromethane + acetone + PLGA^c		21.1 ± 0.8	5.1 ± 0.3

^a 20 mg/mL of PLGA in dichloromethane; ^b 50/50 (v/v) mixture of dichloromethane/acetone; ^c 20 mg/mL of PLGA in 50/50 (v/v) dichloromethane/acetone mixture; na = not applicable due to immediate detachment of the drop; ^d 2.5 mg/mL of PVA in water

Table S3. Interfacial tension values (at 1 min with a drop of 5 µL) of different interfaces involved during the emulsion-evaporation process.

Likewise, without acetone in the organic phase, a measurement in presence of PVA in water was not possible because of the immediate detachment of the droplet from the needle. Indeed, the very rapid and massive adsorption of PVA at the interface led to an interfacial tension decrease below the limit of the instrument. When acetone was present in the organic phase and PVA in the aqueous one, the measurement was possible, demonstrating that acetone played a role in the interfacial properties of the system. This results from the miscibility of acetone and water, contrarily to dichloromethane and water. The process used to prepare PLGA-PVA NPs was thus

not only an emulsion-evaporation, but a combination between emulsion-evaporation² (in which the two liquids are not miscible like dichloromethane and water), nanoprecipitation² (in which the two liquids are miscible like acetone and water) and the Ouzo effect³ (in which the organic phase is composed of two solvents: one miscible with water and the other immiscible). Indeed, when a drop of a 50/50 (v/v) mixture of dichloromethane and acetone was formed in water, the acetone fled from the organic phase into the water, creating a concentration gradient. As PVA is insoluble in acetone, the acetone concentration gradient from the organic phase to the water phase delayed the diffusion of PVA towards the interface, allowing the formation of the droplet. The interfacial tension was then measured at $t = 1$ min after the formation of the droplet, with the detachment of the droplet from the needle occurring at longer times. In any case, the interfacial tension between water and the 50/50 (v/v) mixture of dichloromethane and acetone, was significantly decreased in presence of PVA (from 22.4 ± 0.8 mN/m to 5.2 ± 0.2 mN/m) (Table S3). The PVA chains were thus able to adsorb at the interface contrarily to PLGA ones. Moreover, because PVA is insoluble in organic solvents, it could not be located in the core of the NPs. The 8% (w/w) of PVA chains previously quantified (see Supporting Information 2) in the PLGA-PVA NPs were at the NPs surface. Thus, the PLGA-PVA NP surface was mainly composed of PVA screening the negative charges of PLGA, resulting in approximately neutral NPs, as also observed in zeta potential measurements (see section 3.1. of the main article).

REFERENCES

- (1) Pisani, E.; Fattal, E.; Paris, J.; Ringard, C.; Rosilio, V.; Tsapis, N. Surfactant Dependent Morphology of Polymeric Capsules of Perfluorooctyl Bromide: Influence of Polymer

Adsorption at the Dichloromethane–water Interface. *J. Colloid Interface Sci.* **2008**, 326 (1), 66–71.

- (2) Astete, C. E.; Sabliov, C. M. Synthesis and Characterization of PLGA Nanoparticles. *J. Biomater. Sci. Polym. Ed.* **2006**, 17 (3), 247–289.
- (3) Vitale, S. A.; Katz, J. L. Liquid Droplet Dispersions Formed by Homogeneous Liquid–Liquid Nucleation: “The Ouzo Effect.” *Langmuir* **2003**, 19 (10), 4105–4110.

Supporting Information 4: AFM imaging of the layers of NPs

AFM images of NPs were collected in air at room temperature (22 °C) using a commercial Multimode-8 equipped with a NanoScope V controller from Bruker manufacturer (Bruker, AXS, France). 10 μL of the NP suspension at a concentration of 25 mg/mL were deposited on clean mica surfaces fixed on a magnetic disk directly mounted on top of the AFM scanner. Samples were dried at room temperature for at least 1 h before imaging. Topographical and mechanical properties were imaged using the Peak Force quantitative nano mechanical (QNM) property mode with a nanoindentation frequency of 2 KHz. PeakForce mode worked with small controlled load forces (around 0.1 nN) and with deformation depths as small as 1 nm, so damage to the probe or sample was kept minimal. The elastic modulus was derived from the force curves (by using the Derjaguin-Muller-Toporov (DMT) model). The quantitative mapping of the elastic modulus was performed without irreversible indentation of the sample. MPP-21100-10 cantilevers (Bruker) were calibrated by measuring the thermally-induced motion of an unloaded cantilever. The spring constant was 2.8 N/m (tip radius of about 8 nm). The scan rate was adjusted in the range of 0.5 Hz over selected areas (0.5 μm x 0.5 μm , 1.0 μm x 1.0 μm and 5.0 μm x 5.0 μm). Data processing was performed with the WSxM and Bruker softwares. The Young's modulus was calculated from the AFM images for each type of NPs using the DMT model from the Bruker software. The mean calculated values corresponded to the average of at least 30 measurements obtained from individual NPs and taken from 10 to 15 images for each type of NPs. The roughness was characterized using R_a parameter calculated on 5.0 x 5.0 μm images. R_a is the arithmetic average of the absolute values of the surface height deviations measured from the mean plan.

Topographical (Figure S4) and mechanical (Table S4) properties of dried NPs on clean mica surface were imaged with AFM in air in order *i*) to characterize the surface coverage and roughness after the deposition of NPs on mica before the contact angle measurements and *ii*) to assess the deformability of the NPs through Young's modulus measurements. The mica surface was covered with a dense layer of NPs, as observed in all AFM images (Figure S4).

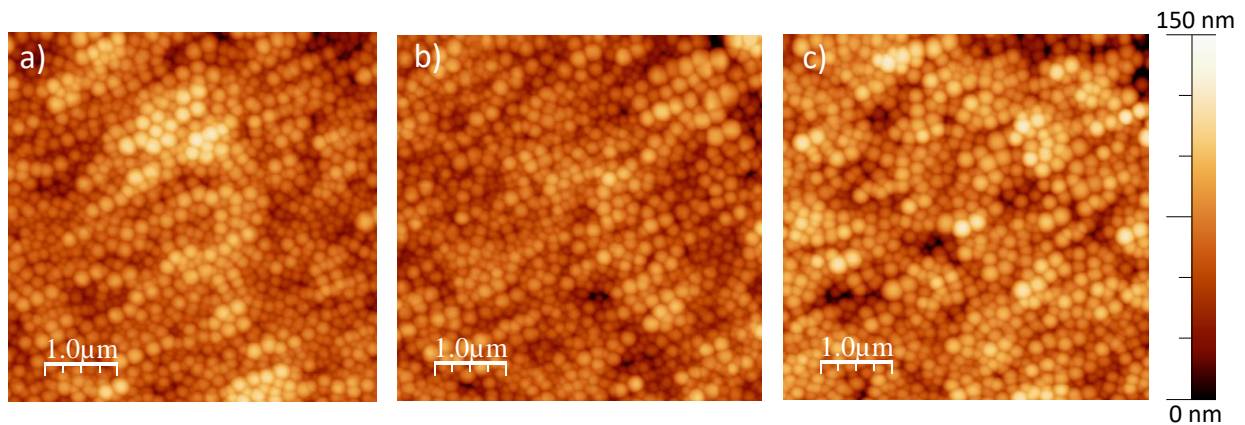


Figure S4. Topographic AFM Images ($5.0 \mu\text{m} \times 5.0 \mu\text{m}$) of dried NPs layer of a) PLGA-PVA NPs b) lyophilized PLGA-PVA NPs and c) PLGA NPs.

NPs	R_a (nm)	Young's modulus (GPa)
PLGA	18 ± 3	4.9 ± 1.3
PLGA-PVA	14 ± 1	9.1 ± 1.8
lyophilized PLGA-PVA	7 ± 2	8.0 ± 1.9

Table S4. Topographical properties of NP layers and mechanical properties of the NPs determined by AFM.

The R_a parameter (Table S4), which characterized the surface roughness, was similar for the layers of PLGA NPs and PLGA-PVA NPs, but it was lower for the layer of lyophilized PLGA-PVA NPs. This could be explained by the additional presence of trehalose in the case of lyophilized NPs which partially filled the interparticular spaces between the NPs once dried. In any case, the R_a parameter indicated a low roughness of the NP layers. The lyophilization process did not affect the Young's modulus of the PLGA-PVA NPs as shown in Table S4. The Young's modulus of the PLGA-PVA NPs (≈ 8 GPa) was twice the one of the PLGA NPs (≈ 4 GPa). These values are consistent with values reported in the literature, with a higher Young's modulus value of a PVA film (≈ 7 GPa)¹ compared to a PLGA film (≈ 3 GPa).² Moreover, the Young's modulus value obtained for PLGA NPs was comparable to those obtained for PLGA films or microparticles². Similarly, the Young's modulus obtained for PLGA-PVA NPs was very close to that obtained for PVA film.¹ As references for example, these NPs are stiffer than polyglycerol based nanogels (between ≈ 1 and 35 MPa)³ but softer than gold NPs (Young's modulus of ≈ 100 GPa).⁴ Consequently, no significant deformation of the core of PLGA-PVA NPs and of PLGA NPs at the oil/water interface was expected, contrarily to what was observed with nanogels.⁵ A similar assumption was made by Gyulai and Kiss with bare PLGA NPs and PLGA NPs sterically stabilized by Pluronic F127.⁶

REFERENCES

- (1) Cadek, M.; Coleman, J. N.; Barron, V.; Hedicke, K.; Blau, W. J. Morphological and Mechanical Properties of Carbon-Nanotube-Reinforced Semicrystalline and Amorphous Polymer Composites. *Appl. Phys. Lett.* **2002**, *81* (27), 5123–5125.

- (2) Sarrazin, B.; Tsapis, N.; Mousnier, L.; Taulier, N.; Urbach, W.; Guenoun, P. AFM Investigation of Liquid-Filled Polymer Microcapsules Elasticity. *Langmuir* **2016**, *32* (18), 4610–4618.
- (3) Rancan, F.; Asadian-Birjand, M.; Dogan, S.; Graf, C.; Cuellar, L.; Lommatzsch, S.; Blume-Peytavi, U.; Calderón, M.; Vogt, A. Effects of Thermoresponsivity and Softness on Skin Penetration and Cellular Uptake of Polyglycerol-Based Nanogels. *J. Controlled Release* **2016**, *228*, 159–169.
- (4) Ramos, M.; Ortiz-Jordan, L.; Hurtado-Macias, A.; Flores, S.; Elizalde-Galindo, J.; Rocha, C.; Torres, B.; Zarei-Chaleshtori, M.; Chianelli, R. Hardness and Elastic Modulus on Six-Fold Symmetry Gold Nanoparticles. *Materials* **2013**, *6* (1), 198–205.
- (5) Schmitt, V.; Destribats, M.; Backov, R. Colloidal Particles as Liquid Dispersion Stabilizer: Pickering Emulsions and Materials Thereof. *Comptes Rendus Phys.* **2014**, *15* (8–9), 761–774.
- (6) Gyulai G., Kiss E., Interaction of poly(lactic-co-glycolic acid) nanoparticles at fluid interfaces, *J. Colloid Interface Sci.* **2017**, *500*, 9-19.

Supporting Information 5: NP hydrophobicity measurements

The NP behavior at the oil/water interface is properly characterized by the three-phase contact angle, but this measurement is very challenging in practice. Indeed, only few techniques are applicable to NPs of about 200 nm,¹ like the gel trapping technique² and the freeze-fracture shadow-casting (FreSCA) cryo-SEM.³ The first method requires a gelling agent (gellan gum) which may modify the interfacial properties of NPs and their distribution at the interface. In our case, this method is also inadequate, since it requires heating at 50–55 °C,² which is above the glass transition temperature of PLGA (45–55 °C).⁴ The second technique (FreSCA cryo-SEM) requires very specific expertise and facilities.

A simpler method would be to measure the contact angle of a water droplet immersed in oil on a NP layer. Unfortunately, a NP layer immersed in water or in oil could not be obtained, as convection movements would take the NPs off the mica surface. NPs could not be attached to the mica surface either, as any product used to attach them would possibly change their interfacial properties. Some authors use a PLGA film instead of a NP layer,^{5,6} but this technique is also not completely representative of the NP behavior at the interface.

For these reasons, we evaluated the NP hydrophobicity by measuring the contact angle of a drop of liquid (water or Miglyol) deposited in the air on top of a NP layer dried onto a mica substrate (see main article Table 2). As seen in AFM pictures, the NP layers covered the substrate as a dense particle layer with a low roughness, similar for PLGA NPs and the non-lyophilized PLGA-PVA

NPs (see Supporting Information 4). However, the liquid might penetrate into the interparticle spaces of the colloidal layer over time, because of the presence of a thick NP layer. Indeed, the number of NP layers could be estimated from the concentration of the NPs (25 mg/mL) in the 45 μ L droplet. With a PLGA NP density of 1.3 g/cm³, a random close packing volume fraction of about 0.65 and a surface area of the mica substrate of 0.8 cm², the height of the NP layer was estimated to \sim 17 μ m, corresponding to a number of NP layers of about 80. This thick NP layer led to an imbibition phenomenon, inducing a decrease of the droplet volume and of the contact angle with time.⁷ This was observed for Miglyol in contact with PLGA NPs or PLGA-PVA NPs, (Figure S5), which is consistent with their low contact angles (Table 2 of main article). The contact angle value was therefore recorded 0.4 s after drop deposit to limit the effect of this imbibition on the measurement. For a droplet of Miglyol on PLGA NPs or PLGA-PVA NPs or for a droplet of water on PLGA-PVA NPs, apparent contact angles were below 90° and indicated good wettability. As the roughness is low (see AFM measurements in Supporting Information 4), it might be assumed that the liquid follows the surface roughness, and that, according to the Wenzel model,⁸ the surface roughness enhanced the wettability. For a droplet of water on PLGA NPs, wettability was poor ($\theta = 120^\circ$). From Butt *et al.*,⁹ the order of magnitude of the maximum pressure that the liquid-vapor interface could stand without having imbibition on a high density layer of particles was estimated at 10⁵ Pa, which was well above the pressure exerted by the droplet of 45 μ L on the interface ($\approx 3 \cdot 10^1$ Pa). Thus, it could be considered that the surface was a mix of solid and air. This case was described by the Cassie or Fakir regime,^{8,9,10} which enhanced the hydrophobicity of the

solid. These “enhancements effects” do not modify the conclusions pertaining to the comparison of the two different types of NPs.

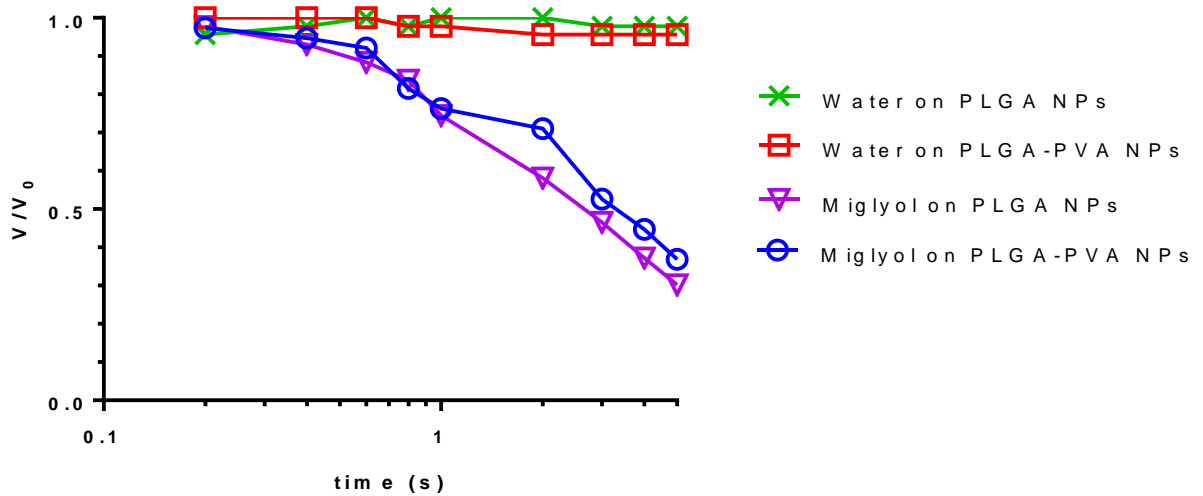


Figure S5. Evolution with time of the droplet volume ratio V/V_0 deposited on a dense PLGA NP or PLGA-PVA NP layer. V is the droplet volume and V_0 is the droplet volume at $t = 0$.

REFERENCES

- (1) Zanini, M.; Isa, L. Particle Contact Angles at Fluid Interfaces: Pushing the Boundary beyond Hard Uniform Spherical Colloids. *J. Phys. Condens. Matter* **2016**, *28* (31), 313002.
- (2) Paunov, V. N. Novel Method for Determining the Three-Phase Contact Angle of Colloid Particles Adsorbed at Air–Water and Oil–Water Interfaces. *Langmuir* **2003**, *19* (19), 7970–7976.
- (3) Isa, L.; Lucas, F.; Wepf, R.; Reimhult, E. Measuring Single-Nanoparticle Wetting Properties by Freeze-Fracture Shadow-Casting Cryo-Scanning Electron Microscopy. *Nat. Commun.* **2011**, *2*:438.

- (4) *Handbook of Pharmaceutical Excipients*, 6. ed.; Rowe, R. C., Ed.; APhA, (PhP) Pharmaceutical Press, 2009.
- (5) Whitby, C. P.; Lim, L. H.; Ghouchi Eskandar, N.; Simovic, S.; Prestidge, C. A. Poly(lactic-Co-Glycolic Acid) as a Particulate Emulsifier. *J. Colloid Interface Sci.* **2012**, 375 (1), 142–147.
- (6) Qi, F.; Wu, J.; Sun, G.; Nan, F.; Ngai, T.; Ma, G. Systematic Studies of Pickering Emulsions Stabilized by Uniform-Sized PLGA Particles: Preparation and Stabilization Mechanism. *J Mater Chem B* **2014**, 2 (43), 7605–7611.
- (7) Shang, J.; Flury, M.; Harsh, J. B.; Zollars, R. L. Comparison of Different Methods to Measure Contact Angles of Soil Colloids. *J. Colloid Interface Sci.* **2008**, 328 (2), 299–307.
- (8) Queré, D. Wetting and roughness, *Annu. Rev. Mater. Res.* **2008**, 38, 71–99.
- (9) Butt, H.-J.; Semprebon C.; Papadopoulos P.; Vollmer D.; Brinkmann M.; Ciccoti M. Design Principles for Superamphiphobic Surfaces. *Soft Matter* **2013**, 9, 418-428.
- (10) Pilat D. W., Papadopoulos P., Schäffel, Vollmer D., Berger R.; Butt H.-J. Dynamic measurement of the Force Required to Move a Liquid Drop on a Solid Surface. *Langmuir* **2012**, 28, 16812-16820.

Supporting Information 6: Examples of Turbiscan curves obtained for the emulsion stabilized by lyophilized PLGA-PVA NPs

An emulsion stabilized by lyophilized PLGA-PVA NPs (NP suspension of 25 mg/mL redispersed in MilliQ water) was prepared, with an aqueous phase/oil phase ratio of 90/10 (w/w) (see main article section 2.4). The emulsion stability was evaluated over 55 days at 25 °C by monitoring the destabilization phenomena using a Turbiscan Classic MA 2000 (Formulation, Toulouse, France) apparatus. The Turbiscan curves allow the identification of the different stages of evolution of the emulsion with time (Figure S6).

An increase of the backscattered light intensity at the bottom of the emulsion layer and a decrease of the backscattered light intensity in the aqueous phase were observed between 0 and 30 min corresponding to a creaming phase (Figure S6a). Between 30 min and 6 h, no evolution of the emulsion was observed as indicated by a perfect overlay of the curves (Figure S6b). Then, the backscattered light intensity on the whole emulsion layer decreased between 6 h and 55 days, corresponding to a flocculation-coalescence step (Figure S6c). Simultaneously, a decrease of the backscattered light intensity in the top of the aqueous phase and an increase in the bottom were noticed, corresponding to the sedimentation of the NPs in excess in the aqueous phase.

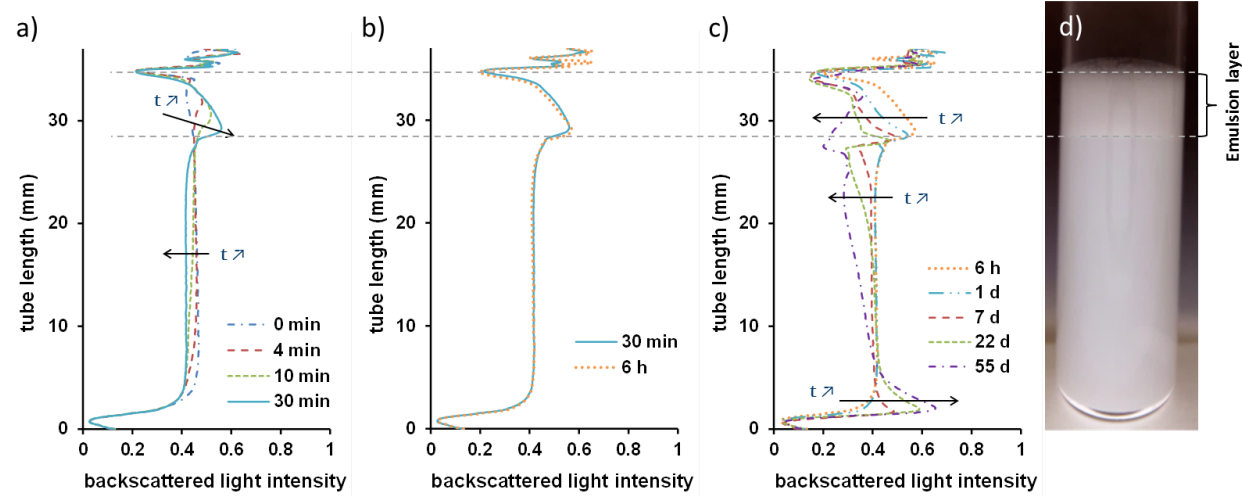


Figure S6. a) to c) Evolution with time of the curves of the backscattered intensity versus tube height for an emulsion of PLGA-PVA NP suspension at 25 mg/mL and Miglyol (ratio 90-10). Example of a) a creaming stage b) a stability stage c) a coalescence-flocculation stage. d) Image at D7 of an emulsion containing 10% (w/w) of Miglyol and 90% (w/w) of lyophilized PLGA-PVA NP suspension at 25 mg/mL in water.

Supporting Information 7: Comparison of the stability of emulsions stabilized either by lyophilized PLGA-PVA NPs, non-lyophilized PLGA-PVA NPs, or trehalose solution

Emulsions were prepared with an aqueous phase/oil phase ratio of 90/10 (w/w) using different aqueous phase: a trehalose solution at 150 mg/mL, a suspension of previously lyophilized PLGA-PVA NPs at a concentration of 25 mg/mL in water or a suspension of non-lyophilized PLGA-PVA NPs at a concentration of 25 mg/mL in water (see main article section 2.4). The stability of the emulsions was evaluated over 55 days at 25 °C by monitoring the destabilization phenomena using a Turbiscan Classic MA 2000. The Turbiscan curves of each emulsion combined with the macroscopic observations performed at the same times allow the construction of the scheme of Figure S7a summarizing the evolution of the emulsion layer for the different formulations.

No difference in stability and in macroscopic structure was noticed between the emulsions stabilized either by lyophilized PLGA-PVA NPs (*i.e.* with trehalose in solution) or by non-lyophilized PLGA-PVA NPs (*i.e.* without trehalose in solution), both in suspension in water at 25 mg/mL (Figure S7b and c). Moreover, the emulsion prepared with trehalose alone in water (150 mg/mL) as the aqueous phase exhibited a poor stability (Figure S7d).

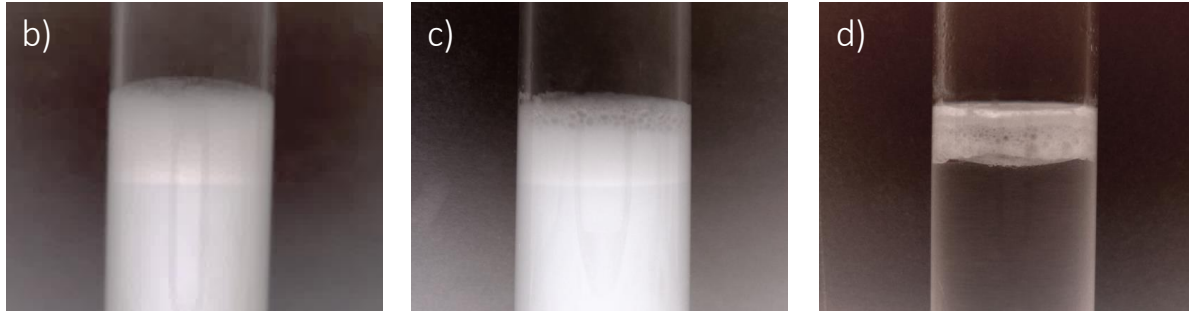
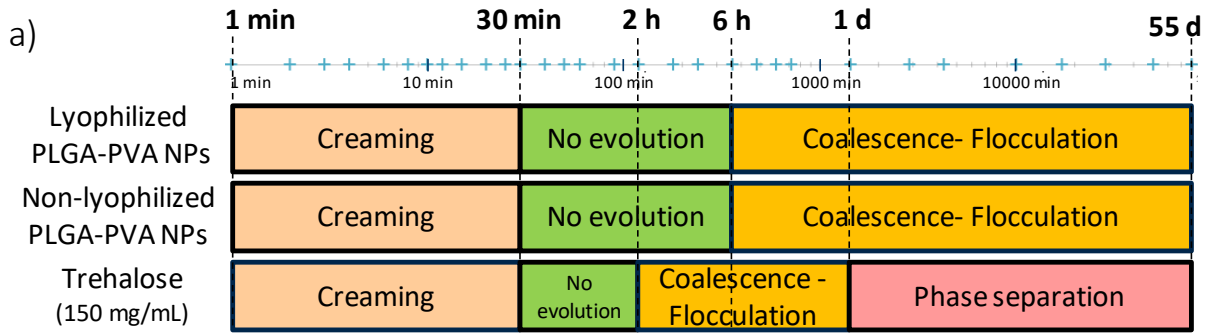


Figure S7. a) Scheme summarizing the evolution of the emulsion layer as determined by Turbiscan analysis for the emulsions, at 90/10 ratio, either with Miglyol and trehalose solution at 150 mg/mL only or stabilized with lyophilized PLGA-PVA NPs or with non-lyophilized PLGA-PVA NPs. Time is indicated on a logarithmic scale. b) to d) Images at D7 of emulsions containing 10% (w/w) of Miglyol and 90% (w/w) of: b) lyophilized PLGA-PVA NP suspension at 25 mg/mL in water; c) non-lyophilized PLGA-PVA NP suspension at 25 mg/mL in water; d) trehalose solution at 150 mg/mL.

Supporting Information 8: Confocal microscopy images of emulsions for different water/oil ratios

Confocal microscopy images of emulsions for different water/oil ratios are provided in Figure S8. Measurements were performed according to the description developed in section 2.5.2 of the main article.

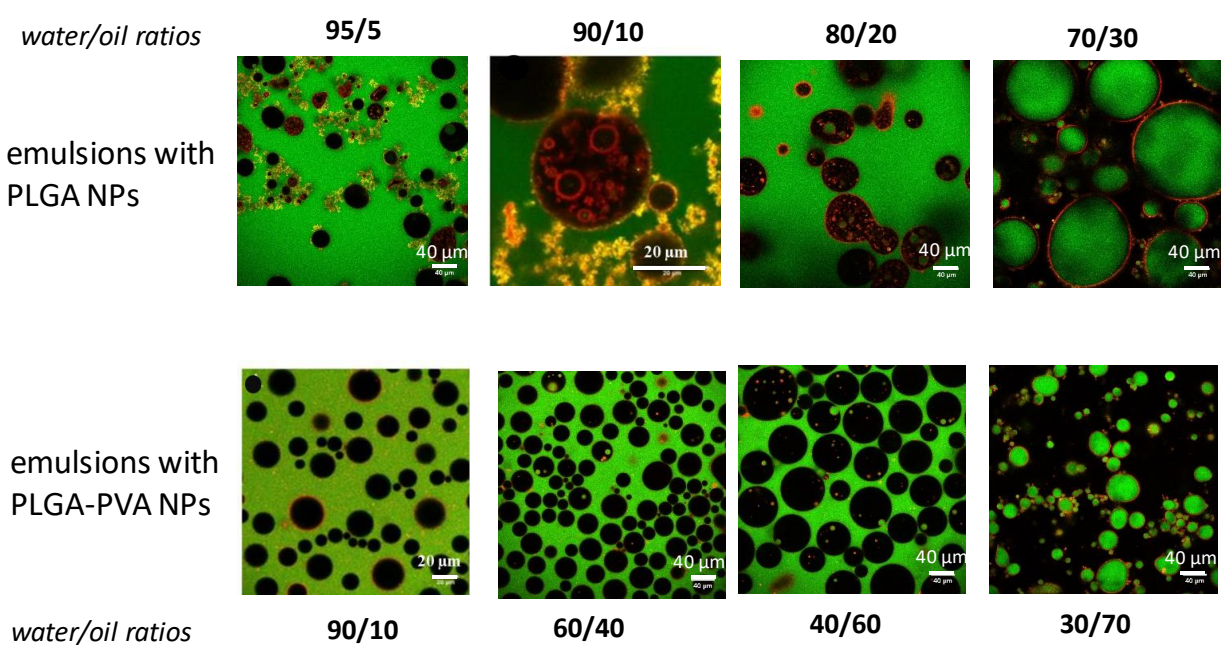


Figure S8. Confocal microscopy images of emulsions (green channel: aqueous phase; red channel: NPs) for different water/oil ratios. Oil phase (Miglyol) was not colored and appeared in black.

With PLGA NPs, multiple W/O/W droplets were obtained for oil ratios ranging from 5 to 20%, below the phase inversion transition occurring at an oil ratio between 20 and 30%. With PLGA-

PVA NPs, O/W emulsions were obtained at an oil ratio of 10%. At ratios ranging between 40 and 60%, multiple droplets could also be observed. The phase inversion was obtained between 60 and 70% of oil. With both types of NPs, the number of multiple droplets progressively increased when approaching the phase inversion. Thus, the proximity of the phase inversion may induce the progressive formation of multiple emulsions, though this does not exclude other explanations such as a three-phase contact angle around 90° or an inherent variation of hydrophobicity among the NPs.

Supporting Information 9: Values of interfacial tension and interfacial moduli at 12 h

The interfacial properties of the NPs at the oil/water interface were investigated with the oscillating pendant drop method. The interfacial tension (γ), the absolute value of the complex dilatational modulus ($|E^*|$) as well as the interfacial elastic (E') and viscous (E'') moduli were recorded over 12 hours. For this purpose, a drop of aqueous phase was formed in Miglyol (see main article sections 2.5.3 and 3.5). The values of γ , $|E^*|$, E' and E'' at 12 hours for all the samples are summarized in Table S9. All the NP suspensions were prepared at a PLGA concentration of 25 mg/mL.

At 12 h	Water	PLGA NPs in water	PLGA NPs in PVA (2 mg/mL)	Non-lyophilized PLGA-PVA NPs in water	PVA solution (2 mg/mL)	Lyophilized PLGA-PVA NPs in water	Non-lyophilized PLGA-PVA NPs in trehalose (150 mg/mL)	Trehalose solution (150 mg/mL)
γ (mN/m)	24.9 ± 0.3	23.0 ± 0.9	17.2 ± 0.6	14.4 ± 0.4	10.8 ± 0.4	8.1 ± 0.3	8.3 ± 0.2	7.4 ± 0.4
$ E^* $ (mN/m)	3.8 ± 0.4	3.6 ± 0.7	3.6 ± 0.2	4.7 ± 0.3	9.1 ± 0.2	3.1 ± 0.1	4.1 ± 0.2	4.1 ± 0.7
E' (mN/m)	3.7 ± 0.4	3.5 ± 0.7	3.5 ± 0.2	4.4 ± 0.3	8.8 ± 0.2	2.9 ± 0.1	3.9 ± 0.2	4.0 ± 0.7
E'' (mN/m)	0.7 ± 0.1	0.8 ± 0.1	1.0 ± 0.1	1.7 ± 0.1	2.4 ± 0.1	1.1 ± 0.1	1.4 ± 0.1	0.9 ± 0.2

Table S9. Interfacial tension, absolute value of the complex dilatational modulus, elastic and viscous moduli of the interface of the different aqueous phases with Miglyol at 12 h. The concentration of the NP suspensions was 25 mg/mL.

Supporting Information 10: Modeling of the adsorption kinetics of NPs at the oil/water interface

To estimate the adsorption energy barrier, we investigated the adsorption kinetics of the NPs at the interface according to a model developed by Bizmark *et al.*¹ and derived from the work of Ward and Tordai.² This model was also used by Nelson *et al.*³ All equations in this Supporting Information come from this model.

At short times ($t \rightarrow 0$), we can consider that a single NP is adsorbed onto a NP-free interface. In such a regime and assuming that there is no energetic adsorption barrier, the adsorption kinetics is governed by a Fickian diffusion, and the interfacial tension γ of NPs vs time t can be fitted with equation 1:

$$\gamma = \gamma_0 - 2N_A C_O |\Delta E_a| \sqrt{\frac{D}{\pi}} \times \sqrt{t} \quad (1)$$

with γ_0 the pristine oil-water interfacial tension, N_A the Avogadro number, C_O the NP bulk concentration, ΔE_a the energy variation of the interface when a single particle is adsorbed (adsorption energy) and D the NP diffusion coefficient in water. The adsorption energy variation ΔE_a was computed from the slope of the linear regression of the interfacial tension as a function of \sqrt{t} at short times, with D determined from Stokes-Einstein equation ($D = k_B T / 6\pi\eta r$), where

k_B is the Boltzmann constant, T the temperature, η the solvent viscosity and r the NP radius (Table S10-1). The fact that $\gamma \propto \sqrt{t}$ indicates that the NP adsorption is indeed controlled by a Fickian diffusion process.

	C_0 (mol/m ³)	D (m ² /s)	$d\gamma/d\sqrt{t}$ (N m ⁻¹ s ^{-1/2})	$ \Delta E_a $ ($k_B T$)
PLGA NPs	1.2×10^{-5}	2.5×10^{-12}	-1.38×10^{-4} $\pm 5.0 \times 10^{-5}$	2.5×10^3 $\pm 0.9 \times 10^3$
PLGA-PVA NPs	6.1×10^{-6}	2.0×10^{-12}	-6.1×10^{-4} $\pm 0.6 \times 10^{-4}$	2.6×10^4 $\pm 0.3 \times 10^3$
lyophilized PLGA-PVA NPs	5.7×10^{-6}	2.0×10^{-12}	-5.7×10^{-4} $\pm 0.2 \times 10^{-4}$	1.2×10^4 $\pm 0.1 \times 10^3$

Table S10-1. NP concentrations, diffusion coefficients (obtained from Stokes-Einstein equation), slopes of Eq 1 and estimated NP adsorption energy variations for PLGA NPs, PLGA-PVA NPs and lyophilized PLGA-PVA NPs.

At long times ($t \rightarrow \infty$), NPs already adsorbed at the interface slow the adsorption flux, since their interfacial organization must be rearranged to let others NP to be adsorbed. For these later stages of adsorption, the NP interfacial tension can be described by equation 2:

$$\gamma = \gamma_\infty + \frac{K_1 |\Delta E_a|}{(\pi r^2)^2 N_A C_0 \sqrt{D}} \times \frac{1}{\sqrt{t}} \quad (2)$$

with γ_∞ the interfacial tension at long times (saturated interface) and K_1 a dimensionless constant, which can be related to the adsorption constant k_a with equation 3:

$$k_a = \frac{\theta^3}{4.64 K_1^2} \times DN_A C_O \pi r^2 \quad (3)$$

with θ the interfacial coverage (fraction of the interface covered by the NPs; we take $\theta = 0.91$, corresponding to a close-packed interface).⁴

The adsorption energy barrier ϕ_b for a single NP resulting from NP-interface interactions of different nature (e.g. electrostatic, hydrophobic, Van der Waals) can finally be computed from k_a with equation 4.

$$k_a \cong \frac{D}{R} \sqrt{\frac{\phi_b}{\pi k_B T}} \exp\left(-\frac{\phi_b}{k_B T}\right) \quad (4)$$

Values for ϕ_b are reported in Table S10-2.

	$d\gamma/d(1/\sqrt{t})$ (N m ⁻¹ s ^{1/2})	K_1 (-)	k_a (m/s)	ϕ_b ($k_B T$)
PLGA NPs	1.3×10^{-1} $\pm 0.5 \times 10^{-1}$	7.5×10^1 $\pm 4.6 \times 10^1$	1.2×10^{-11} $\pm 0.1 \times 10^{-11}$	15 ± 1
PLGA-PVA NPs	6.0×10^{-2} $\pm 0.2 \times 10^{-2}$	7.7 ± 2.2	1.5×10^{-9} $\pm 0.6 \times 10^{-9}$	10 ± 1
lyophilized PLGA-PVA NPs	4.2×10^{-2} $\pm 0.1 \times 10^{-2}$	13.5 ± 1.4	0.5×10^{-9} $\pm 0.3 \times 10^{-9}$	11 ± 1

Table S10-2. Slope of Eq 2, dimensionless constant K_1 , adsorption constant k_a and adsorption energy barrier ϕ_b for PLGA NPs, PLGA-PVA NPs and lyophilized PLGA-PVA NPs.

We found that ϕ_b is higher than the average kinetic thermal energy: the adsorption was slowed down by the adsorption energy barrier, which was higher for bare PLGA NPs than for PLGA-PVA NPs (lyophilized or not). This could be explained by the higher zeta potential of bare PLGA NPs, inducing stronger particle-interface repulsion, with interfaces already covered by charged NPs.^{5,6} However, $\phi_b \ll |\Delta E_a|$: the adsorption energy barrier is very small compared to the adsorption energy. Thus, the interface can be considered as barrier-free.^{1,3}

REFERENCES

- (1) Bizmark, N.; Ionnidis, M. A.; Henneke, D. E. Irreversible Adsorption-Driven Assembly of Nanoparticles at Fluid Interfaces Revealed by a Dynamic Surface Tension Probe. *Langmuir* **2014**, 30, 710-717.
- (2) Ward A. F. H.; Tordai L. Time-Dependence of Boundary Tensions of Solutions I. The Role of Diffusion in Time-Effects. *J. Chem. Phys.* **1946**, 14, 453-461.
- (3) Nelson, A.; Wang, D.; Koynov, K.; Isa, L. A Multiscale Approach to the Adsorption of Core-shell Nanoparticles at Fluid Interfaces. *Soft Matter* **2015**, 11, 118–129.

- (4) Du K.; Glogowski E.; Emrick T.; Russell T. P. ; Dinsmore A. D. Adsorption Energy of Nano- and Microparticles at Liquid-Liquid Interfaces. *Langmuir* **2010**, 26, 12518-12522.
- (5) Gyulai G., Kiss E., Interaction of poly(lactic-co-glycolic acid) nanoparticles at fluid interfaces, *J. Colloid Interface Sci.* **2017**, 500, 9-19.
- (6) Dugyala, V. R.; Muthukuru J. S.; Mani E.; Basavaraj M. G. Role of electrostatic interactions in the adsorption kinetics of nanoparticles at fluid–fluid interfaces. *Phys. Chem. Chem. Phys.* **2016**, 18, 5499

Supporting Information 11: Measurement of the critical aggregation concentration (CAC) of PVA

PVA aqueous solutions from 10^2 to 10^{-5} mg/mL were prepared by dilution of a PVA stock solution at 10^2 mg/mL. The surface tension of these solutions was measured at 20 °C by the Wilhelmy plate method, using a thermostated automatic digital tensiometer (model Krüss K10T, Germany). Prior to the experiments, the surface of the solutions was cleaned using an absorbing paper. Then, the platinum plate of the tensiometer was brought into contact with the solution surface and the surface tension was measured until its value was considered as stable. The accuracy of the force transducer of the tensiometer was 0.1 mN/m. The reported values of surface tensions at equilibrium in Figure S11 are the average of at least two measurements. The curve of the surface tension at equilibrium versus PVA concentration was plotted on a semi-logarithmic scale.

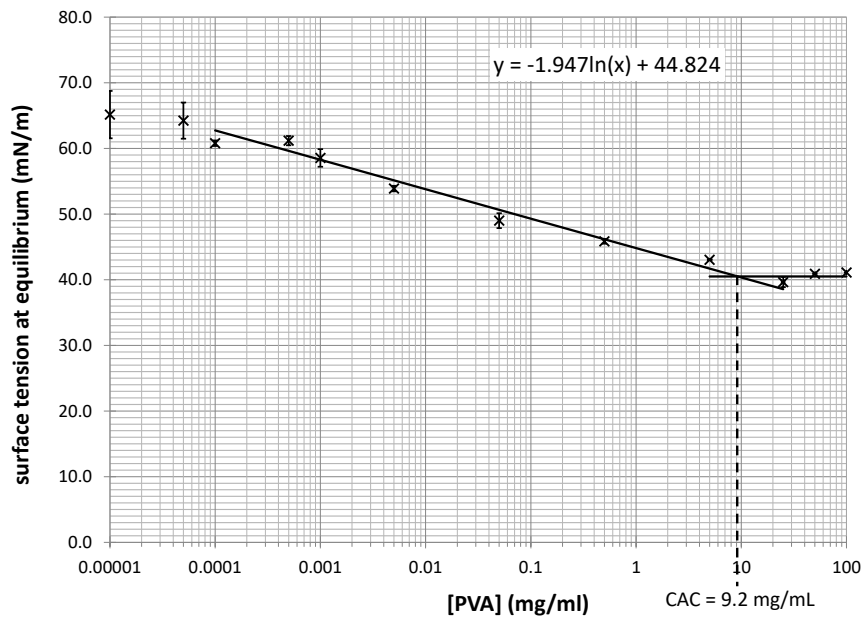


Figure S11. Plot of the surface tension at equilibrium versus PVA concentration in order to determine the CAC of PVA.

The CAC of PVA was determined at 9.2 mg/mL as the concentration above which the surface tension at equilibrium reaches a plateau.¹ All the PVA aqueous solutions prepared in this study had a concentration lower than the CAC: there was no aggregate of PVA in these solutions.

REFERENCE

- (1) Diamant, H.; Andelman, D. Onset of Self-Assembly in Polymer-Surfactant Systems. *EPL Europhys. Lett.* **1999**, *48* (2), 170.